Biol. Cybern. 61, 255–264 (1989)

Biological Cybernetics

Central Adaptation Models of the Vestibulo-Ocular and Optokinetic Systems

J. M. R. Furman[1], T. C. Hain[2], and G. D. Paige[3]

[1] Department of Otolaryngology, University of Pittsburgh, Pittsburgh, Pa, USA
[2] Department of Neurology, Johns Hopkins University, Baltimore, Md, USA
[3] Department of Otolaryngology, Washington University, St. Louis, Mo, USA

Abstract. A theoretical analysis of two models of the vestibulo-ocular and optokinetic systems was performed. Each model contains a filter element in the vestibular periphery to account for peripheral adaptation, and a filter element in the central vestibulo-optokinetic circuit to account for central adaptation. Both models account for *1* adaptation, i.e. a response decay to a constant angular acceleration input, in both peripheral vestibular afferent and vestibulo-ocular reflex (VOR) responses and *2* the reversal phases of optokinetic after-nystagmus (OKAN) and the VOR and *3* oscillatory behavior such as periodic alternating nystagmus. The two models differ regarding the order of their VOR transfer function. Also, they predict different OKAN patterns following a prolonged optokinetic stimulus. These models have behavioral implications and suggest future experiments.

Introduction

The vestibulo-ocular reflex (VOR) acts to maintain the orientation of the eyes such that visual targets remain stable on the retina during head movement. However, during constant velocity head movements in the dark, eye velocity is equal and opposite to head velocity for only a few seconds because eye velocity decays toward zero. The pattern with which eye velocity declines has prompted the development of many mathematical models of vestibular signal processing. Early models of the VOR used a mathematical form developed for the peripheral vestibular apparatus, i.e. the "torsion pendulum model" of semicircular canal cupular movement (see Wilson and Jones 1979). These models predicted that the response, in terms of slow component eye velocity, to a brief angular acceleration of the head would consist primarily of a decaying exponential. Such models did not predict the decay of response seen during sustained acceleratory stimuli (Boumans et al. 1983; Brown and Wolfe 1969; Malcolm and Jones 1970; Paige 1983a) nor the reversal in direction that follows the previously mentioned exponential decay in the VOR response to brief angular acceleration (Sills et al. 1978; Aschan and Bergstedt 1955; Jeannerod et al. 1975). Subsequent models of the VOR accounted for these behaviors by the inclusion of an "adaptation operator" (Young and Oman 1969; Malcolm and Jones 1970; Schmid et al. 1971). These operators stored signals in the path between the inner ear and the eye muscles and, because their contents were subtracted from the unadapted output, caused the response decline and undershoot behaviors mentioned above.

Shown in Fig. 1 are block diagrams, based on work by Young and Oman (1969) and Malcolm and Jones (1970), of two models of the VOR that contain adaptation operators. Although the models in Fig. 1

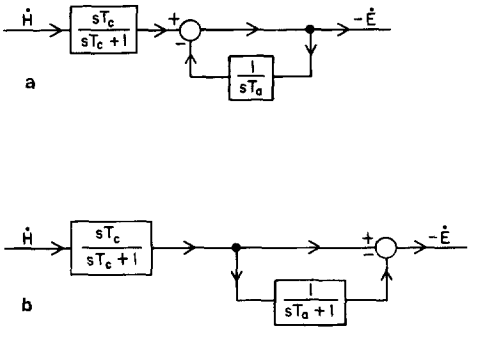

Fig. 1a and b. Vestibulo-ocular reflex models that include adaptation operators. **a** Based on work by Young and Oman (1969). Note that a negative feedback loop is used to create the adaptation operator. **b** Based on work by Malcolm and Jones (1970). Note that a negative feed-forward loop is used to create the adaptation operator. In both models, s is the Laplace operator, $\dot{E}$ is eye velocity, $\dot{H}$ is head velocity, T_c is the cupular time constant, and T_a is the adaptation time constant

differ from one another, both have the identical VOR transfer function:

$$\frac{\dot{E}}{\dot{H}} = \frac{-sT_c}{sT_c+1} \cdot \frac{sT_a}{sT_a+1}, \tag{1}$$

where $\dot{E}$ is eye velocity, $\dot{H}$ is head velocity, T_c is the long peripheral vestibular time constant, and T_a is the adaptation time constant. This transfer function is characteristic of a second order overdamped system (Hostetter et al. 1982). In other words, the impulse response of $\dot{E}$ can be expressed as the sum of two decaying exponentials. Because their transfer functions are identical, the models in Fig. 1 make identical predictions of behavior. Accordingly, both models account for VOR response decline following prolonged constant angular acceleration and for the reversal in direction of vestibular nystagmus that occurs following brief, unidirectional rotational accelerations. These models do not address the question of whether the adaptation process occurs in peripheral vestibular (inner ear and eighth cranial nerve) or central vestibular (brain stem and cerebellum) structures.

Subsequent models of the VOR accounted for not only adaptation but also for the known association between vestibular and optokinetic responses (Waespe and Henn 1977a, b). These models employed shared VOR and optokinetic processing with feedforward (Raphan et al. 1977) or feedback (Robinson 1977) circuits. These models also included a distinction between peripheral vestibular afferent and central vestibular processing and thereby accounted for the difference in dynamics between peripheral vestibular firing patterns in primary afferents and VOR responses.

A representative vestibulo-optokinetic model is shown in Fig. 2. The transfer function of this model with switch $S1$ open, relating $\dot{E}$ to $\dot{H}$ is:

$$\frac{\dot{E}}{\dot{H}} = \frac{-1}{1-k} \cdot \frac{sT_c}{sT_c+1} \cdot \frac{sT_a}{sT_a+1} \cdot \frac{sT_0+1}{sT_0/(1-k)+1}, \tag{2a}$$

where k is the central loop gain. It can be simplified by matching the time constant of the central vestibulo-optokinetic circuit, T_0, to the peripheral vestibular (cupular) time constant T_c. Then, a pole-zero cancellation is effected (Robinson 1981) so that the VOR transfer function is:

$$\frac{\dot{E}}{\dot{H}} = \frac{-1}{1-k} \cdot \frac{sT_a}{sT_a+1} \cdot \frac{sT_c}{sT_v+1}, \tag{2b}$$

where $T_v = T_c/(1-k)$ is the behavioral VOR time constant. In this way, despite cascading a second order vestibular periphery with a first order central vestibulo-optokinetic system (which results in a third order system), by appropriate choice of T_0, the model reduces to second order VOR dynamics overall. Optokinetic after-nystagmus (OKAN), a persistent nystagmus in darkness following optokinetic stimulation (modelled by opening the switch $S1$), is also generated by this model and is predicted to decay with the same time constant as that of the VOR, namely $T_c/(1-k)$. The model thus accounts for the fact that the time constant of the VOR and that of OKAN are similar and that these time constants exceed the time constant of peripheral vestibular afferents, as $T_c/(1-k) > T_c$, for $0 < k < 1$. Note that because the adaptation operator, $sT_a/(sT_a+1)$, is located in the vestibular periphery, the model accounts for adaptation in both peripheral vestibular afferents and the VOR. However, because the model shown in Fig. 2 is overdamped it cannot account for oscillatory behaviors that have been observed in the VOR (Baloh et al. 1976; Hood 1981; Jung and Kornhuber 1964). Furthermore, because the central portion of the model is first order, it cannot account for oscillatory behavior in optokinetic responses, i.e. the reversal phases of OKAN (e.g. OKAN II) (Aschan and Bergstedt 1955; Brandt et al. 1974; Büttner et al. 1976; Koerner and Schiller 1972; Waespe and Henn 1978). These observations could be explained by postulating a *central* adaptation operator.

Additional support for a central adaptation operator comes from habituation paradigms, i.e. repeated exposure to optokinetic or rotational stimula-

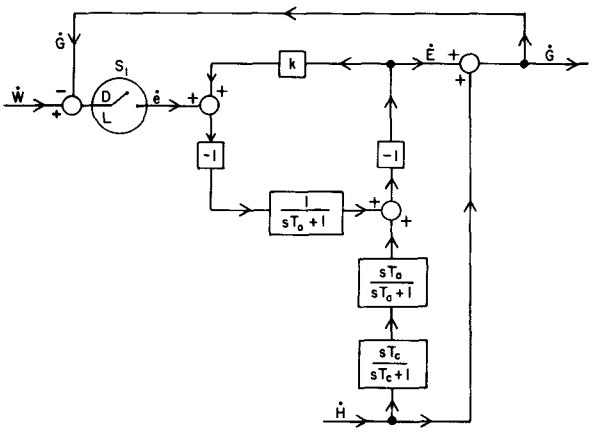

Fig. 2. A combined model of the vestibular and optokinetic systems based on work by Robinson (1977). The peripheral vestibular system is modeled by both a cupular time constant, T_c, and an adaptation time constant, T_a. The central nervous system is modeled as a positive feedback loop containing a low pass filter with time constant T_0 and loop gain k. Parameters are as in Fig. 1 and $\dot{G}$ is gaze velocity, $\dot{W}$ is the velocity of the world with respect to the subject, and $\dot{e}$ is retinal slip velocity. The switch $S1$, represents the visual condition with D ($S1$ open) indicating darkness and L ($S1$ closed) indicating a lighted visual surround

tion. Optokinetic habituation results in a shorter OKAN duration and an increase in the peak velocity of OKAN II (Waespe and Henn 1978). Such changes in optokinetic responses are readily accounted for by the presence of a central adaptation operator whose characteristics can be altered. Habituation to rotational stimulation is characterized by an earlier onset of post-rotatory nystagmus reversal and an increase in low frequency phase lead (Buettner et al. 1981; Paige 1983b). Such changes in VOR responses have been accounted for by alterations in both the long VOR time constant and in the adaptation time constant (Buettner et al. 1981; Paige 1983b). In that peripheral vestibular adaptation is unlikely to be changed by repeated stimulation, the presence of a central (modifiable) adaptation operator is thus likely.

In an effort to simulate the ocular motor disorder of periodic alternating nystagmus (PAN) (Baloh et al. 1976), an extreme case of oscillatory behavior, Leigh et al. (1981), developed a model that included an adaptation operator in the central vestibulo-optokinetic system. The Leigh et al. (1981) model is identical to that shown in Fig. 3a except that their model did not include the peripheral adaptation operator (which is enclosed by dashed lines). Contrary to the model in Fig. 2, which contains a second order vestibular periphery and a first order central vestibulo-optokinetic system, the Leigh et al. (1981) model has a first order vestibular periphery and a second order central vestibular system. Like Robinson (1981), Leigh et al. (1981) matched the central time constant, T_0, to the peripheral vestibular (cupular) time constant, T_c, to effect a pole-zero cancellation so that the VOR transfer function of the model in Fig. 3, omitting peripheral adaptation, is:

$$\frac{\dot{E}}{\dot{H}} = \frac{-sT_c \cdot sT_{ac}}{T_c \cdot T_{ac} \cdot s^2 + (T_{ac} - k \cdot T_{ac} + T_c) \cdot s + 1}, \quad (3)$$

where $1/T_{ac}$ is the gain of the central negative feedback loop. Thus, despite cascading a first order vestibular periphery with a second order central vestibulo-optokinetic system, the VOR transfer function of the Leigh et al. (1981) model reduces to second order dynamics. Because of second order dynamics in the central vestibulo-optokinetic system, by appropriate choice of T_{ac} and loop gain k, the model can account for reversal phases of OKAN, and, with the addition of appropriate nonlinearities, can account for PAN. Maioli (1988) has recently proposed a model of OKAN that also uses second-order central dynamics. Both the Leigh et al. (1981) and the Maioli (1988) models, however, ignore adaptation in peripheral vestibular responses. In this regard, it is known that at least part of the adaptation process is peripheral in that response decline and reversal phases have been observed in eighth nerve recordings (Goldberg and Fernandez 1971; Blanks et al. 1975).

Based on the model shown in Fig. 2 and the model of Leigh et al. (1981), we endeavored to develop an improved model of the vestibular and optokinetic systems that accounts for adaptation in both peripheral vestibular afferent and VOR responses, as well as oscillatory phenomena in the vestibular and optokinetic systems.

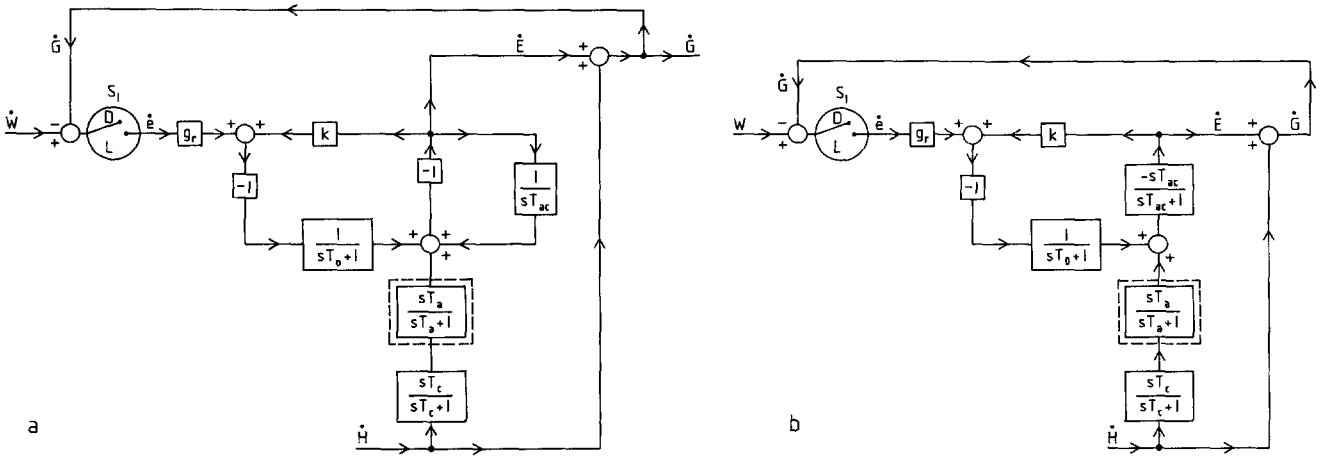

Fig. 3a and b. A model of the vestibular and optokinetic systems that contains both a peripheral vestibular afferent and a central vestibular adaptation operator. Removal of the element surrounded by dashed lines results in the model proposed by Leigh et al. (1981). **a** A model with a positive and a negative feedback loop in the central nervous system. **b** Block reduction of **a** with a single central nervous system loop containing a high pass filter element. Designations are as in Figs. 1 and 2, T_{ac} is the central adaptation time constant, and g_r is the retinal slip gain

Model Development

Two alternative models of the vestibulo-optokinetic system were evaluated. Each of these models, one shown in Fig. 3 and one shown in Fig. 4, includes an adaptation operator in both the peripheral vestibular and the central vestibulo-optokinetic systems. The model in Fig. 3a can be viewed as the Leigh et al. (1981) model with the addition of a peripheral adaptation operator. This model, written in block reduced form (Fig. 3b), can also be viewed as the model of Fig. 2 with the addition of an adaptation operator, $sT_{ac}/(sT_{ac}+1)$, to the central vestibulo-optokinetic loop. The model in Fig. 4 was developed by modifying the central adaptation operator of Fig. 3 for reasons to be discussed below. These models were analyzed in terms of their ability to simulate observed vestibular and optokinetic phenomena.

The model in Fig. 3 accounts for adaptation phenomena in both peripheral and central vestibular responses and it predicts oscillatory behavior in VOR and OKAN responses. The VOR transfer function of the model (with switch $S1$ open) is

$$\frac{\dot{E}}{\dot{H}} = \frac{-sT_c}{sT_c+1} \cdot \frac{sT_a}{sT_a+1} \times \frac{(sT_0+1)\cdot(sT_{ac})}{T_0 \cdot T_{ac} \cdot s^2 + (T_{ac} - k \cdot T_{ac} + T_0)\cdot s + 1}. \quad (4)$$

By setting T_0 equal to T_c, the VOR transfer function reduces to

$$\frac{\dot{E}}{\dot{H}} = \frac{-sT_a}{sT_a+1} \times \frac{s^2 \cdot T_c \cdot T_{ac}}{T_c \cdot T_{ac} \cdot s^2 + (T_{ac} - k \cdot T_{ac} + T_c)\cdot s + 1}, \quad (5)$$

which is characterized by third order dynamics. This complexity in response dynamics results from the cascading of a second order vestibular periphery with a second order central vestibulo-optokinetic system and cancellation of only a single pole.

Using the standard form

$$\frac{\dot{E}}{\dot{H}} = \frac{sT_a}{sT_a+1} \cdot \frac{-s^2}{s^2+2\zeta\omega_n s+\omega_n^2} \quad (6)$$

the behavior of the model in Fig. 3 can be described as that of a peripheral adaptation operator cascaded with a second order system with a damping ratio ζ of

$$\zeta = (T_c + T_{ac}\cdot[1-k])/(2\cdot[T_c \cdot T_{ac}]^{1/2}) \quad (6a)$$

and a characteristic frequency ω_n of

$$\omega_n = 1/(T_c \cdot T_{ac})^{1/2}. \quad (6b)$$

Note that this is a third transfer function. However, for large T_{ac} (>1000), the central adaptation operator becomes ineffective and the model reduces to that of Fig. 2. Because T_0 has been chosen to equal T_c and because the values of T_c and T_a are known from vestibular afferent data, the only undetermined parameters in the transfer function are the loop gain k and the central adaptation time constant T_{ac}.

Shown in Fig. 5a is a diagram of the VOR behavior of the model in Fig. 3 as a function of the values of k and T_{ac}. It can be seen that by appropriate choice of the model parameters, the system will either *1* have all real poles ($\zeta > 1$), i.e. be overdamped, *2* contain two complex conjugate poles ($\zeta < 1$), i.e. be underdamped, or *3* have right half-plane poles ($\zeta < 0$), i.e. be unstable. The $T_{ac} - k$ regions that produce these behaviors are separated by lines that define critically damped ($\zeta = 1$) and

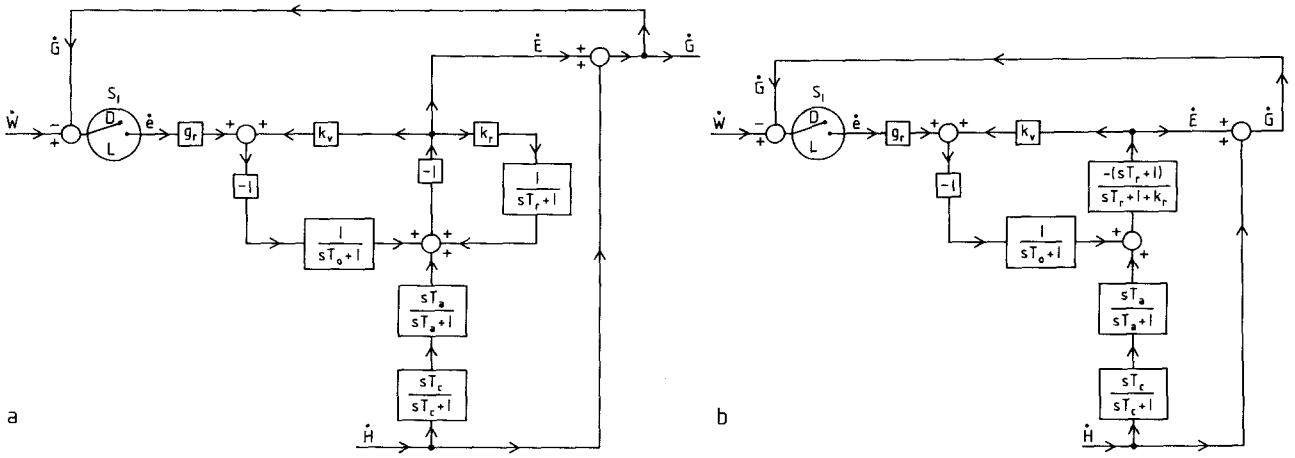

Fig. 4a and b. An alternative model of the vestibular and optokinetic systems that contains both a peripheral vestibular afferent and a central vestibular adaptation operator. **a** A model with a positive and a negative feedback loop in the central nervous system. **b** Block reduction of **a** with a single central nervous system loop containing a lead-lag element. Designations are as in Figs. 1 and 2, k_r and k_v are loop gains, T_r is the central adaptation time constant, and g_r is the retinal slip gain

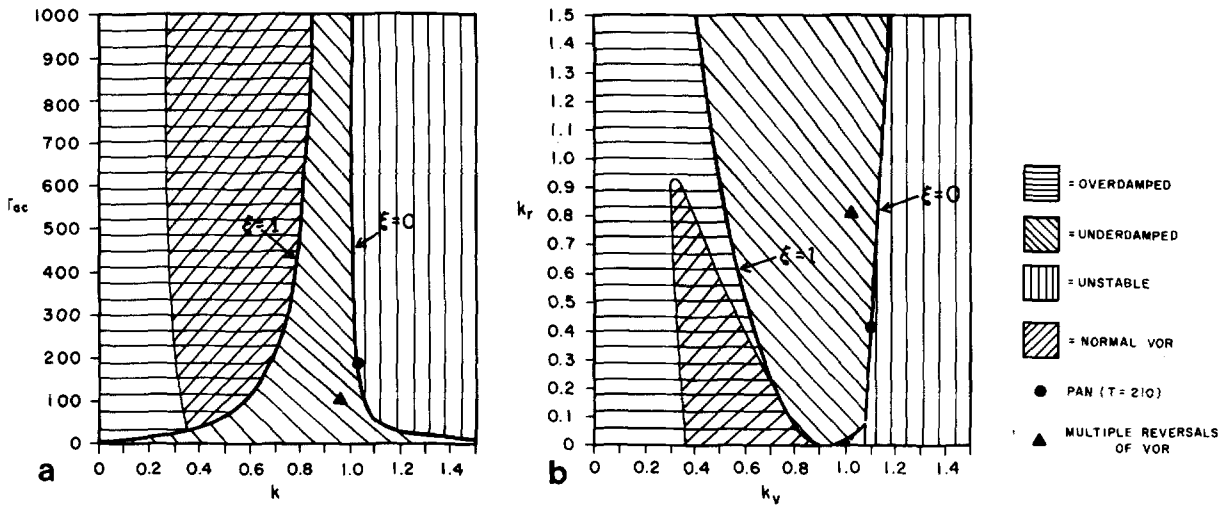

Fig. 5a and b. Dependence of model behavior on parameter values. **a** Behavior of model shown in Fig. 3 as loop gain k and central adaptation time constant, T_{ac}, are varied to yield different types of second order dynamics. $T_0 = T_c = 5.7$ s. **b** Behavior of model shown in Fig. 4 as loop gains k_r and k_v are varied to yield different types of second order dynamics. $T_0 = T_c = 5.7$ s. $T_r = T_a = 80$ s. The parameter value regions that correspond to normal VOR behavior are indicated. Also shown are the parameter combinations used to simulate the eye movement velocity of a patient with periodic alternating nystagmus and the VOR response to a step in head velocity of a patient with rebound nystagmus reported by Hood (1981)

undamped ($\zeta = 0$) responses. The parameter region producing VOR responses that are within normal limits is also indicated on Fig. 5a. This region is based on the results of Malcolm and Jones (1970) who used the overdamped second order VOR model shown in Fig. 1b to characterize the VOR responses of normal subjects. Because the model in Fig. 3 has third order VOR dynamics, pole locations could not be matched directly. Rather, the region of normality in Fig. 5a was generated by matching the VOR phase leads predicted by the model in Fig. 3 at 0.01 and 0.05 Hz to the phase leads predicted by the model in Fig. 1b using the VOR response parameters developed by Malcolm and Jones (1970).

The model in Fig. 3 predicts that OKAN is described by (see Appendix):

$$\dot{E}_{\mathrm{OKAN}}(t) = \mathscr{L}^{-1}\left[\frac{-\dot{W}\cdot g_r}{T_0}\cdot\frac{1}{s^2+2\zeta\omega_n s+\omega_n^2}\right], \tag{7}$$

where $\mathscr{L}^{-1}$ indicates the inverse Laplace transform, and ζ and ω_n are as in (6). Note that OKAN dynamics are predicted to have the same dependence on model parameters as those of the VOR (see Fig. 5a).

In an effort to simplify the overall VOR transfer function of the model in Fig. 3, the adaptation operator was changed by substituting a leaky integrator $1/(sT_r+1)$ for the ideal central integrator, $1/s$, of Fig. 3a. This substitution results in the model of Fig. 4. It can be seen in the block reduced form of the model that the adaptation operator is changed from the high pass filter, $sT_{ac}/(sT_{ac}+1)$, of Fig. 3b to the lead-lag network, $(sT_r+1)/(sT_r+1+k_r)$, of Fig. 4b, where T_r is the time constant of the central adaptation operator, and k_r is the gain of the central negative feedback loop.

The model in Fig. 4 has a VOR transfer function of

$$\frac{\dot{E}}{\dot{H}} = \frac{-sT_c}{sT_c+1}\cdot\frac{sT_a}{sT_a+1}\cdot\frac{(sT_0+1)\cdot(sT_r+1)}{T_0\cdot T_r\cdot s^2+(T_r-k_v\cdot T_r+T_0+k_r\cdot T_0)\cdot s+(1-k_v+k_r)}, \tag{8}$$

where k_v is the gain of the central positive feedback loop. By setting the time constant of the central adaptation operator, T_r, equal to that of the peripheral adaptation operator, T_a, a pole-zero cancellation can be effected in a manner analogous to the matching of T_0 to T_c as discussed above. Thus, with T_0 equal to T_c, and T_r equal to T_a, the transfer function reduces to

$$\frac{\dot{E}}{\dot{H}} = \frac{-s^2\cdot T_c\cdot T_a}{T_c\cdot T_a\cdot s^2+(T_a-k_v\cdot T_a+T_c+k_r\cdot T_c)\cdot s+(1-k_v+k_r)}, \tag{9}$$

which is that of a second order dynamic system. Therefore, despite cascading a second order vestibular periphery with a second order central vestibular system, the VOR transfer function reduces to that of a second order system overall and thus conforms to existing descriptions of VOR responses. The model in Fig. 4 accounts for adaptation phenomena in both peripheral and central vestibular responses. Also, with appropriate choice of parameters, the model can produce oscillatory behavior in VOR and OKAN responses.

Using the form

$$\frac{\dot{E}}{\dot{H}} = \frac{-s^2}{s^2 + 2\zeta\omega_n s + \omega_n^2} \tag{10}$$

the VOR behavior of the model in Fig. 4 can be described as that of a second order system with a damping ratio ζ of

$$\zeta = (T_c \cdot [1 + k_r] + T_a \cdot [1 - k_v])/(2 \cdot [T_c \cdot T_a \cdot (1 - k_v + k_r)]^{1/2}) \tag{10a}$$

and a characteristic frequency ω_n of

$$\omega_n = ([1 - k_v + k_r]/[T_c \cdot T_a])^{1/2}. \tag{10b}$$

Because T_0 has been chosen to equal T_c, and T_r has been chosen to equal T_a, (T_c and T_a known from vestibular afferent data), the only undetermined parameters in the transfer function are the loop gains k_v and k_r. Shown in Fig. 5b is a diagram of the model's VOR behavior as a function of the values of k_v and k_r. It can be seen that by appropriate choice of the loop gains, the system will either *1* have real poles ($\zeta > 1$), i.e. be overdamped, *2* have complex conjugate poles ($\zeta < 1$), i.e. be underdamped, or *3* have right half-plane poles ($\zeta < 0$) i.e. be unstable. The $k_v - k_r$ regions that produce these behaviors are separated by lines that define critically damped ($\zeta = 1$) and undamped ($\zeta = 0$) responses. The region of loop gain combinations that produce VOR responses that are within normal limits also is indicated on Fig. 5. This region was generated using the data of Malcolm and Jones (1970) noted above, in which they used the overdamped second order VOR model shown in Fig. 1b to characterize normal subjects. Because the model in Fig. 4 has second order VOR dynamics, pole locations could be matched directly to those developed by Malcolm and Jones (1970).

The model in Fig. 4 predicts that OKAN is described by (see appendix):

$$\dot{E}_{OKAN}(t) = \mathscr{L}^{-1}\left[\frac{g_r \cdot \dot{W}}{1 + g_r - k_v + k_r} \cdot \frac{s + 2\zeta\omega_n - T_r \cdot \omega_n^2}{s^2 + 2\zeta\omega_n s + \omega_n^2}\right], \tag{11}$$

where $\mathscr{L}^{-1}$ indicates the inverse Laplace transform, and ζ and ω_n are as in (10). Note that OKAN dynamics are predicted to have the same dependence on model parameters as that of the VOR (see Fig. 5b).

Using the models shown in Figs. 3 and 4, we simulated *1* normal behavior including adaptation in VOR responses and OKAN with reversal phases, and *2* abnormal behavior including a damped oscillatory VOR response and PAN. The locations of the parameter combinations used for these simulations are shown in Fig. 5. Figure 6 shows simulated normal VOR adaptation and simulated normal OKAN using the model of Fig. 4. Figure 7a shows simulated damped oscillatory VOR responses using the model of Fig. 4; Model parameters were chosen to reproduce the VOR responses of a patient with rebound nystagmus described by Hood (1981).

To simulate PAN, the loop gain k (for the model of Fig. 3) or k_v (for the model of Fig. 4) was modeled using a nonlinearity such that its value decreased exponentially from a nominal value as eye velocity increased. That is, the loop gain was of the form $(k_{max} - k_{min}) \cdot \exp(-|\dot{E}|/\dot{E}_0) + k_{min}$, where k_{max} is the nominal loop gain at zero eye velocity, k_{min} is the

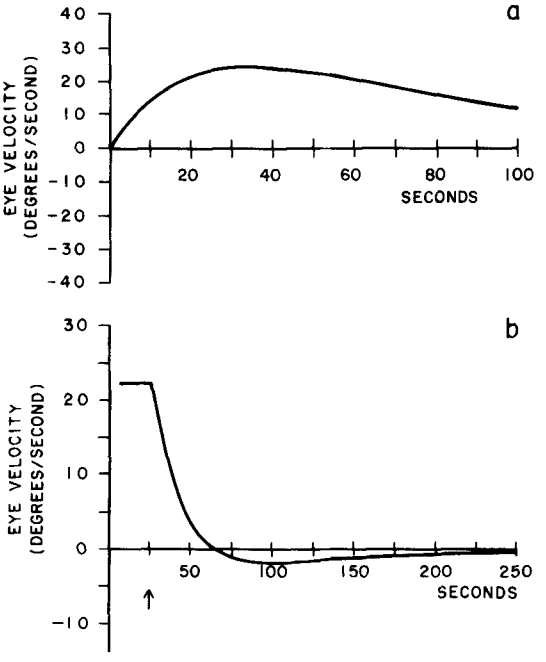

Fig. 6. a Simulated slow component eye velocity of normal response decline during a rotational VOR stimulus of constant acceleration. The model shown in Fig. 4 was used with parameter values of $T_0 = T_c = 5.7$; $T_r = T_a = 80$; $k_v = 0.7$; $k_r = 0.05$; $\dot{H}(t) = 2t$; Switch *S1* open. **b** Simulated slow component eye velocity of OKAN with a reversal phase. The model shown in Fig. 4 was used with parameter values of $T_0 = T_c = 5.7$; $T_r = T_a = 80$; $k_v = 0.7$; $k_r = 0.05$; $g_r = 1.0$; $\dot{W}(t) = 30$; $\dot{H}(t) = 0$. The arrow indicates the time at which switch *S1* was opened (after steady state)

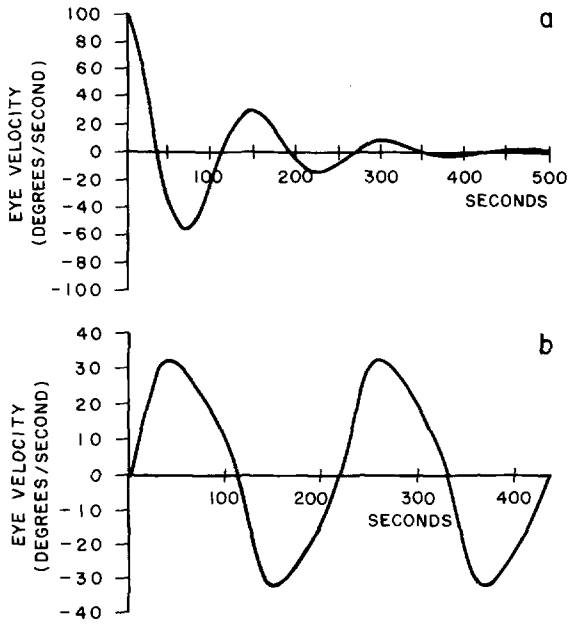

Fig. 7. a Simulated slow component eye velocity of the VOR response to a step in head velocity of a patient reported by Hood (1981) with rebound nystagmus. The model shown in Fig. 4 was used with parameter values of $T_0 = T_c = 5.7$; $T_r = T_a = 80$; $k_v = 1.03$; $k_r = 0.8$; $g_r = 1.0$; $\dot{H}(t) = 100$; switch $S1$ open. **b** Simulated slow component eye velocity of a patient with periodic alternating nystagmus. The model shown in Fig. 4 was used with parameter values of $T_0 = T_c = 5.7$; $T_r = T_a = 80$; $k_v = 1.4 \exp(-|\dot{E}|/45) + 0.2$; $k_r = 0.52$; $g_r = 1.0$; $\dot{H}(t) = 0$; switch $S1$ open

minimum loop gain at large eye velocity, and $\dot{E}_0$ is a scale factor. This nonlinearity was included so that the system would oscillate and yet remain stable (Hostetter et al. 1982). By appropriate choice of T_{ac} and nominal k values or of k_r and nominal k_v values, the oscillation frequency could be made to equal the typical oscillation frequency of PAN, i.e. about 0.005 Hz. The location of the parameter combinations used to simulate PAN are shown as filled circles in Fig. 5. A simulation of the slow component eye velocity during PAN using the model shown in Fig. 4 is shown in Fig. 7b.

Model Comparison

The models shown in Figs. 3 and 4 are characterized by third order and second order VOR transfer functions respectively. However, when using parameter values that enable the model to simulate the responses of normal subjects (see Fig. 5), the responses of these two models are virtually indistinguishable except at low frequencies of stimulation, i.e. in the range of 0.01 Hz or below.

The difference between the two models can best be appreciated by considering OKAN dynamics. The model in Fig. 4 predicts that a prolonged optokinetic stimulus will result in a non-zero steady state charging of the central vestibulo-optokinetic system. Such a prolonged stimulus to the model of Fig. 3 will result in a zero steady state condition (although steady state eye velocity will be non-zero if the pursuit system is considered). Data from both man and rhesus monkey suggest that a prolonged (several minute) optokinetic stimulus causes OKAN of short duration and reduced velocity followed by OKAN II (Brandt et al. 1974; Büttner et al. 1976). This finding supports the validity of the models in Figs. 3 and 4, both of which predict such a reduction in OKAN velocity and duration as the stimulus duration is increased. However, the model in Fig. 3 predicts that the onset of OKAN II will occur immediately upon the cessation of a prolonged optokinetic stimulus, a behavior that has only been reported in labyrinthine defective humans (Zee et al. 1976) and subjects exposed to 15 min of constant velocity optokinetic stimulation with the eyes kept stationary by fixation (Brandt et al. 1974). Neither model includes the nonlinearities that could account for saturation of optokinetic responses or the nonlinearities that could account for the increase in OKAN II following brief exposure to a stationary full field visual surround (Waespe et al. 1978).

A difference in the two models' ability to store central vestibulo-optokinetic activity would be expected for any constant central input such as that which may be produced by a prolonged caloric irrigation (Baertschi et al. 1975; Bock et al. 1979). The continuous nystagmus produced by prolonged caloric irrigation supports the validity of the model in Fig. 4, which predicts a non-zero steady state eye velocity.

Both models suggest that persons should exist whose post-rotatory responses are a damped oscillation rather than simply an exponential decay with an undershoot. Hood (1981) and Jung and Kornhuber (1964), in fact, have reported patients who had such underdamped responses. A simulation of one of these patients' responses is shown in Fig. 7a. Using large amplitude rotational stimuli, more of these individuals may be identified.

Both models can be written as containing either double or single loop central vestibulo-optokinetic structures. That is, "block reduced" equivalents of the central circuitry can be drawn. Although the form in which a model is written does not have any implication regarding its correctness mathematically, any attempt to attach structural neurophysiological significance to a model may depend on the form in which it is written. In this sense, the double loop models suggest the existence of a central negative feedback loop in addition to the positive feedback loop postulated in previous models (Robinson 1977; Leigh et al. 1981).

The single loop models suggest that adaptation may occur within the positive feedback loop itself, for example, by high pass filtering effects occurring in the vestibular nuclei at either a membrane or a synaptic level.

Conclusion

We have presented two models of the vestibulo-optokinetic systems that incorporate a central adaptation operator in addition to the well established and analogous peripheral adaptation operator. These adaptation operators account for both the response decay in peripheral neurons to constant stimulation, response decay in central neurons to constant central stimulation, as well as oscillatory behaviors such as PAN and the reversal phases of OKAN.

Appendix

Figure 8 is a simplified feedback control system representing the optokinetic reflex, where the reference input is the velocity of the optokinetic stimulus, $\dot{W}$; the output is eye velocity, $\dot{E}$; and the error signal, $\dot{e}$, equals retinal slip velocity, when switch $S1$ is closed. For a step input of optokinetic stimulus velocity, i.e. $\dot{W}(s)=\dot{W}\cdot 1/s$ with $S1$ closed, where s is the Laplace operator, the slow component optokinetic eye velocity, $\dot{E}_{OKN}(t)$, is characterized by

$$\dot{E}_{OKN}(t)=\mathscr{L}^{-1}\left[\frac{\dot{W}}{s}\cdot\frac{G(s)}{1+G(s)}\right], \tag{A1}$$

where $\mathscr{L}^{-1}$ denotes the inverse Laplace transform and $G(s)$ denotes the open loop optokinetic transfer function. Extinguishing the optokinetic stimulus to generate OKAN is equivalent to opening the switch $S1$, i.e. setting the error, $\dot{e}(t)$, to zero. The slow component OKAN eye velocity, $\dot{E}_{OKAN}(t)$, can be calculated by including non-zero initial conditions in the analysis of the open loop optokinetic system with a zero error velocity as input. This is accomplished by first determining the differential equation that relates $\dot{E}(t)$ to $\dot{e}(t)$ from the inverse Laplace transform of the open loop optokinetic transfer function $G(s)$. Then, this differential equation is Laplace transformed using the initial conditions $\dot{E}(0^-)$ and $\dot{e}(0^-)$ and the constraint that $\dot{e}(s)=0$. $\dot{E}_{OKAN}(t)$ is then calculated using inverse Laplace transforms.

For the model shown in Fig. 3, the open loop optokinetic reflex transfer function $G(s)$ is given by

$$G(s)=\frac{g_r}{T_0\cdot T_{ac}}\cdot\frac{sT_{ac}}{s^2+2\zeta\omega_n s+\omega_n^2}, \tag{A2}$$

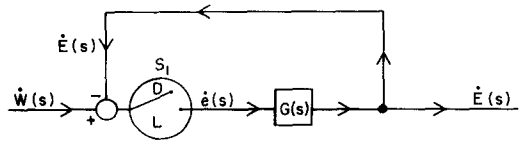

Fig. 8. Simplified diagram of the optokinetic system. Note that the contribution of the pursuit system is not included. $G(s)$ represents the open loop optokinetic reflex transfer function. Designations as in Figs. 1 and 2

where

$$\zeta=(T_0+T_{ac}\cdot[1-k])/(2\cdot[T_0\cdot T_{ac}]^{1/2}) \tag{A2a}$$

and

$$\omega_n=1/(T_0\cdot T_{ac})^{1/2}. \tag{A2b}$$

Thus, for a step input, $\dot{W}\cdot 1/s$, of the optokinetic stimulus, using (A1), the slow component optokinetic eye velocity, $\dot{E}_{OKN}(t)$, is characterized by

$$\dot{E}_{OKN}(t)=\mathscr{L}^{-1}\left[\frac{\dot{W}}{s}\cdot\frac{g_r}{T_0}\cdot\frac{s}{s^2+2\zeta'\omega_n s+\omega_n^2}\right], \tag{A3}$$

where

$$\zeta'=(T_0+T_{ac}\cdot[1+g_r-k])/(2\cdot[T_0\cdot T_{ac}]^{1/2}) \tag{A3a}$$

and

$$\omega_n=1/(T_0\cdot T_{ac})^{1/2}. \tag{A3b}$$

At steady state, using the final value theorem, the slow component optokinetic eye velocity, $\dot{E}_{OKN}(t)$, will have a value of zero, and the steady state error velocity, $\dot{e}(t)$, will thus equal the stimulus velocity $\dot{W}$. If the optokinetic stimulus is extinguished at some time t prior to reaching steady state, the dynamics of the resulting output depends on that time t, and it is impractical to generate analytically an expression for $\dot{E}_{OKAN}(t)$. However, if the optokinetic stimulus is extinguished after $\dot{E}_{OKN}(t)$ has attained a value of zero, the slow component OKAN eye velocity $\dot{E}_{OKAN}(t)$, for the model in Fig. 3, will equal

$$\dot{E}_{OKAN}(t)=\mathscr{L}^{-1}\left[\frac{-\dot{W}\cdot g_r}{T_0}\cdot\frac{1}{s^2+2\zeta\omega_n s+\omega_n^2}\right], \tag{A4}$$

where ζ and ω_n are as in (A2).

Note that this OKAN response, $\dot{E}_{OKAN}(t)$, depends on the value of ζ. For $\zeta>1$, $G(s)$ has real poles and the OKAN eye velocity $\dot{E}_{OKAN}(t)$ is given by

$$\dot{E}_{OKAN}(t)=\frac{\dot{W}\cdot g_r}{T_0}\cdot\frac{1}{b-a}\cdot[\exp(-at)-\exp(-bt)], \tag{A5}$$

where ζ and ω_n are as in (A2), and

$$a=\omega_n\cdot(\zeta+[\zeta^2-1]^{1/2}), \tag{A5a}$$

$$b=\omega_n\cdot(\zeta-[\zeta^2-1]^{1/2}). \tag{A5b}$$

For $\zeta<1$, $G(s)$ has complex conjugate poles and the eye velocity $\dot{E}_{OKAN}(t)$ is given by

$$\dot{E}_{OKAN}(t)=\frac{-\dot{W}\cdot g_r}{T_0\cdot\omega_n\cdot(1-\zeta^2)^{1/2}}\cdot\exp(-\zeta\omega_n t)\times \mathrm{SIN}[\omega_n\cdot(1-\zeta^2)^{1/2}\cdot t], \tag{A6}$$

where ζ and ω_n are as in (A2).

Note that the initial optokinetic eye velocity will be negative following a prolonged optokinetic stimulus to the model of Fig. 3.

For the model shown in Fig. 4, the open loop optokinetic reflex transfer function $G(s)$ is given by

$$G(s)=\frac{g_r}{T_0\cdot T_r}\cdot\frac{sT_r+1}{s^2+2\zeta\omega_n s+\omega_n^2}, \tag{A7}$$

where

$$\zeta=(T_0\cdot[1+k_r]+T_r\cdot[1-k_v])/(2\cdot[T_0\cdot T_r\cdot(1-k_v+k_r)]^{1/2}) \tag{A7a}$$

and

$$\omega_n=([1-k_v+k_r]/[T_0\cdot T_r])^{1/2}. \quad \text{(A7b)}$$

Thus, for a step input, $\dot{W}\cdot 1/s$, of the optokinetic stimulus, using (A1), the slow component optokinetic eye velocity, $\dot{E}_{OKN}(t)$, is characterized by

$$\dot{E}_{OKN}(t)=\mathscr{L}^{-1}\left[\frac{\dot{W}}{s}\cdot\frac{g_r}{T_0\cdot T_r}\cdot\frac{sT_r+1}{s^2+2\zeta'\omega_n's+\omega_n'^2}\right], \quad \text{(A8)}$$

where

$$\zeta'=(T_0\cdot[1+k_r]+T_r\cdot[1+g_r-k_v])/(2\cdot[T_0\cdot T_r\cdot(1+g_r-k_v+k_r)]^{1/2}) \quad \text{(A8a)}$$

and

$$\omega_n'=([1+g_r-k_v+k_r]/[T_0\cdot T_r])^{1/2}. \quad \text{(A8b)}$$

$\dot{E}_{OKN}(t)$, at steady state, using the final value theorem, will have a nonzero value of $\dot{W}\cdot g_r/(1+g_r-k_v+k_r)$. The steady state error velocity, $\dot{e}(t)$, will thus equal $\dot{W}\cdot(1-k_v+k_r)/(1+g_r-k_v+k_r)$. Therefore, if the optokinetic stimulus is extinguished after a steady state condition is reached, using the method described above, the slow component OKAN eye velocity, $\dot{E}_{OKAN}(t)$, for the model in Fig. 4, is given by:

$$\dot{E}_{OKAN}(t)=\mathscr{L}^{-1}\left[\frac{g_r\cdot\dot{W}}{1+g_r-k_v+k_r}\cdot\frac{s+2\zeta\omega_n-T_r\cdot\omega_n^2}{s^2+2\zeta\omega_n s+\omega_n^2}\right], \quad \text{(A9)}$$

where ζ and ω_n are as in (A7).

Now, the OKAN response, $\dot{E}_{OKAN}(t)$, depends on the value of ζ. For $\zeta>1$, $G(s)$ has real poles and the slow component OKAN eye velocity $\dot{E}_{OKAN}(t)$ is given by

$$\dot{E}_{OKAN}(t)=\frac{g_r\cdot\dot{W}}{1+g_r-k_v+k_r}\times\left[\frac{(1-a\cdot T_r)\cdot b}{b-a}\exp(-at)-\frac{(1-b\cdot T_r)\cdot a}{b-a}\exp(-bt)\right], \quad \text{(A10)}$$

where ζ and ω_n are as in (A7), and,

$$a=\omega_n\cdot(\zeta+[\zeta^2-1]^{1/2}), \quad \text{(A10a)}$$

$$b=\omega_n\cdot(\zeta-[\zeta^2-1]^{1/2}). \quad \text{(A10b)}$$

For $\zeta<1$, $G(s)$ has complex conjugate poles and the slow component OKAN eye velocity $\dot{E}_{OKAN}(t)$ is given by

$$\dot{E}_{OKAN}(t)=\frac{g_r\cdot\dot{W}\cdot(1-2\cdot\omega_n\cdot T_r\cdot\zeta+T_r\cdot\omega_n)}{(1+g_r-k_v+k_r)\cdot(1-\zeta^2)^{1/2}}\times\exp(-\zeta\omega_n t)\cdot\mathrm{COS}(\omega_d\cdot t+\Phi), \quad \text{(A11)}$$

where ζ and ω_n are as in (A7), and

$$\omega_d=\omega_n\cdot(1-\zeta^2)^{1/2}, \quad \text{(A11a)}$$

and

$$\Phi=\mathrm{TAN}^{-1}[(T_r\cdot\omega_n-\zeta)/(1-\zeta^2)^{1/2}]. \quad \text{(A11b)}$$

Acknowledgements. The authors wish to thank Dr. Edward Kamen for helpful suggestions and Karen Chianelli for typing the manuscript. This work was supported by NIH grants NS25700 (JF), EY05505 (Th), and AG06442 (GP).

References

Aschan G, Bergstedt M (1955) The genesis of secondary nystagmus induced by vestibular stimuli. Acta Soc Med Upsaliensis 60:113–122

Baertschi AJ, Johnson RN, Hanna GR (1975) A theoretical and experimental determination of vestibular dynamics in caloric stimulation. Biol Cybern 20:175–186

Baloh RW, Honrubia V, Konrad HR (1976) Periodic alternating nystagmus. Brain 99:11–26

Blanks RHI, Estes MS, Markham CH (1975) Physiologic characteristics of vestibular first order canal neurons in the cat. II. Response to constant angular acceleration. J Neurophysiol 38:1250–1268

Bock O, Koschitzky HV, Zangemeister WH (1979) Vestibular adaptation to long-term stimuli. Biol Cybern 33:77–79

Boumans LJJM, Rodenburg M, Maas AJJ (1983) Response of the human vestibulo-ocular reflex system to constant angular acceleration. II. Experimental investigation. ORL 45:130–142

Brandt TH, Dichgans J, Buchele W (1974) Motion habituation: Inverted self-motion perception and optokinetic after-nystagmus. Exp Brain Res 21:337–352

Brown JH, Wolfe JW (1969) Adaptation to prolonged constant angular acceleration. Acta Otolaryngol 67:389–398

Büttner UW, Waespe W, Henn V (1976) Duration and direction of optokinetic after-nystagmus as a function of stimulus exposure time in the monkey. Arch Psychiatr Nervenkr 222:281–291

Büttner UW, Henn V, Young LR (1981) Frequency response of the vestibulo-ocular reflex (VOR) in the monkey. Aviat Space Environ Med 52:73–77

Goldberg JM, Fernandez C (1971) Physiology of peripheral neurons innervating semicircular canals of the squirrel monkey. I. Resting discharge and response to constant angular accelerations. J Neurophysiol 34:635–660

Hood JD (1981) Further observations on the phenomenon of rebound nystagmus. Ann NY Acad Sci 374:532–539

Hostetter GH, Savant CJ, Stefani RT (1982) Design of feedback control systems. Holt, Rinehart, and Winston, New York

Jeannerod M, Magnin M, Schmid R, Stefanelli M (1975) Vestibular habituation to angular velocity steps in the cat. Biol Cybern 22:39–48

Jung R, Kornhuber HH (1964) Results of electronystagmography in man: the value of optokinetic, vestibular, and spontaneous nystagmus for neurologic diagnosis and research. In: Bender MB (ed) The oculomotor system. Harper and Row, New York, pp 428–488

Koerner F, Schiller PH (1972) The optokinetic response under open and closed loop conditions in the monkey. Exp Brain Res 14:318–330

Leigh RJ, Robinson DA, Zee DS (1981) A hypothetical explanation for periodic alternating nystagmus: instability in the optokinetic-vestibular system. Ann NY Acad Sci 374:619–635

Maioli C (1988) Optokinetic nystagmus: modeling the velocity storage mechanism. J Neurosci 8:821–832

Malcolm R, Jones GM (1970) A quantitative study of vestibular adaptation in humans. Acta Otolaryngol 70:126–135

Paige GD (1983a) Vestibuloocular reflex and its interactions with visual following mechanisms in the squirrel monkey. I. Response characteristics in normal animals. J Neurophysiol 49:134–151

Paige GD (1983b) Vestibuloocular reflex and its interactions with visual following mechanisms in the squirrel monkey. II. Response characteristics and plasticity following unilateral inactivation of horizontal canal. J Neurophysiol 49:152–168

Raphan T, Cohen B, Matsuo V (1977) A velocity storage mechanism responsible for optokinetic nystagmus (OKN), optokinetic after-nystagmus (OKAN) and vestibular nystagmus. In: Baker R, Berthoz A (eds) Control of gaze by brain stem neurons. Elsevier/North-Holland Biomedical Press, New York

Robinson DA (1977) Vestibular and optokinetic symbiosis: an example of explaining by modelling. In: Baker R, Berthoz A (eds) Control of gaze by brain stem neurons. Elsevier/North-Holland Biomedical Press, New York

Robinson DA (1981) The use of control systems analysis in the neurophysiology of eye movements. Ann Rev Neurosci 4:463–503

Schmid R, Stefanelli M, Mira E (1971) Mathematical modelling. A contribution to clinical vestibular analysis. Acta Otolaryngol 72:292–302

Sills AW, Honrubia V, Baloh RW (1978) Is the adaptation model a valid description of the vestibulo-ocular reflex? Biol Cybern 30:209–220

Waespe W, Henn V (1977a) Neuronal activity in the vestibular nuclei of the alert monkey during vestibular and optokinetic stimulation. Exp Brain Res 27:523–538

Waespe W, Henn V (1977b) Vestibular nuclei activity during optokinetic after-nystagmus (OKAN) in the alert monkey. Exp Brain Res 30:323–330

Waespe W, Henn V (1978) Reciprocal changes in primary and secondary optokinetic after-nystagmus (OKAN) produced by repetitive optokinetic stimulation in the monkey. Arch Psychiatr Nervenkr 225:23–30

Waespe W, Huber Th, Henn V (1978) Dynamic changes of optokinetic after-nystagmus (OKAN) caused by brief visual fixation periods in monkey and in man. Arch Psychiatr Nervenkr 226:1–10

Wilson VJ, Jones GM (1979) Mammalian vestibular physiology. Plenum Press, New York

Young LR, Oman CM (1969) Model for vestibular adaptation to horizontal rotation. Aerosp Med 40:1076–1080

Zee DS, Yee RD, Robinson DA (1976) Optohiuetic responses in labyrintline-defective human beings. Brain Res 113:423–428

Received: October 18, 1988
Accepted: February 2, 1989

Dr. Joseph M. R. Furman
Department of Otolaryngology, Suite 500
Eye and Ear Institute of Pittsburgh
203 Lothrop Street
Pittsburgh, PA 15213
USA